Published in final edited form as:
J Immunol. 2009 September 1; 183(5): 3364–3372. doi:10.4049/jimmunol.0900641.

Memory-Like CD8+ T Cells Generated during Homeostatic Proliferation Defer to Antigen-Experienced Memory Cells[1]

Kitty P. Cheung, **Edward Yang**, and **Ananda W. Goldrath**[2]
University of California, San Diego, Division of Biological Sciences, La Jolla, CA 92093

Abstract

Naive T cells proliferate in response to lymphopenia and acquire the phenotypic and functional qualities of memory T cells, providing enhanced protection against infection. How well memory-like T cells generated during lymphopenia-induced homeostatic proliferation (HP)-memory differentiate into secondary memory cells and compete with Ag-experienced true-memory cells is unknown. We found that $CD8^+$ HP-memory T cells generated robust responses upon infection and produced a secondary memory population comparable to true-memory cells in the absence of competition. However, when true-memory and HP-memory T cells competed during infection, HP-memory cells contributed less to the effector population, contracted earlier, and formed fewer secondary memory cells. Furthermore, HP- and true-memory cells demonstrated distinct chemokine receptor expression and localization within the spleen during infection, indicating differential access to signals necessary for secondary memory formation. Thus, HP-memory T cells provide protection without compromising the true-memory population. Differences in HP- and true-memory T cells may reveal the basis of competition for limited resources within the memory-T cell compartment.

During acute infection, pathogen-specific $CD8^+$ T cells are induced to undergo extensive proliferation and differentiation into cytolytic T lymphocytes able to eliminate infected cells. Following the clearance of infection, a portion of these Ag-specific lymphocytes seed the memory compartment, often providing the host with enhanced protection against a subsequent encounter with that same pathogen. Memory $CD8^+$ T cells mediate control of secondary infections due to their higher precursor frequency, rapid reacquisition of effector function, and access to peripheral sites of infection. $CD8^+$ T cell memory can be remarkably stable, providing life-long protection in some cases (1). What mechanisms regulate the different T cell subsets within the memory T cell compartment and how heterogeneous populations of memory T cells change over time are not well elucidated.

Ag-independent proliferation of T cells occurs when lymphocyte numbers drop below a certain threshold (2–4). This lymphopenia-induced expansion of lymphocytes is known as homeostatic proliferation (HP),[3] which is one mechanism contributing to the restored T cell homeostasis.

[1]This work was supported by grants from the National Institutes of Health (R01AI67545), Cancer Research Institute, and Pew Scholars Program (A.W.G.), the University of California, San Diego Cellular and Molecular Genetics Training Grant (K.P.C.) and the Chancellor's Research Scholarship (E.Y.).

2 Address correspondence and reprint requests to Dr. Ananda W. Goldrath, University of California, San Diego, Division of Biological Sciences, 9500 Gilman Drive, La Jolla, CA 92093-0377. agoldrath@ucsd.edu.

Disclosures
The authors have no financial conflict of interest.

[3]Abbreviations used in this paper: HP, homeostatic proliferation; DC, dendritic cell; Lm.OVA, recombinant *Listeria monocytogenes* expressing ovalbumin; MZ, marginal zone; OVAp, peptide derived from $OVA_{(257–264)}$; PALS, periarteriolar lymphoid sheath; qPCR, quantitative PCR; RP, red pulp.

HP allows the remaining peripheral T cell specificities to regenerate the diminished lymphocyte compartment. HP can be caused by radio- or chemotherapy, viral infections such as HIV, and postnatal lymphopenia (5). Surprisingly, naive $CD8^+$ T cells that undergo HP progressively acquire the phenotypic and functional characteristics of memory T cells. This includes the expression of activation markers such as CD44, CD122, CD127, and Ly6C and the ability to rapidly make cytokines such as IFN-γ and lyse-infected cells upon stimulation (2,3,6). These memory-phenotype cells generated by HP provide comparable protection against bacterial infection in vivo as Ag-experienced $CD8^+$ T cells (6), showing that they are a good surrogate for true-memory cells. The HP-memory gene-expression pattern (7) and dependence on $CD4^+$ T cell help for functional protection (6) also serve to emphasize their similarity to Ag-experienced memory cells.

The ability to induce immunological memory independent of infection represents significant therapeutic potential. This may be particularly advantageous for immunocompromised individuals, as the benefit of a rapid response to Ag could compensate for low lymphocyte numbers. Additionally, the enhanced activity of cells undergoing HP has been shown to improve anti-tumor responses (5,8). Conversely, the gain of functional activity associated with HP has proven to be a barrier for acceptance of transplanted tissues (9) and has been implicated in the induction of autoimmunity (5).

To understand the benefits or dangers of HP-induced memory formation, it is important to consider how cells compete for limited space and resources. Competition between memory T cells of different specificities can result in the attrition of previously formed memory (10), but the nature of the recall response evoked by HP- and true-memory subsets with the same specificity was not known. In this study, we examined how these two distinct memory subsets respond to secondary infection. Importantly, we found that these two memory populations make equivalent responses when they represented the sole memory T cell subset, but when in competition with one another, the true-memory T cells dominated the response and formed more secondary memory. Interestingly, this defect by the HP-memory cells could not be rescued by addition of exogenous cytokines or excess Ag. Furthermore, the HP-memory cells showed disorganized trafficking patterns within the spleen, indicating that HP-memory cells may fail to receive the necessary signals to form secondary memory cells efficiently.

Materials and Methods

Mice and adoptive transfers

All mouse work was performed in an Assessment and Accreditation of Laboratory Animal Care-accredited facility according to the University of California San Diego Institutional Animal Care and Use Guidelines. C57BL/6J (B6) mice were obtained from The Jackson Laboratory and bred in our facility along with CD45.1 and CD45.1.2 congenic mice on a B6 background. OT-I $RAG^{-/-}$ TCR-transgenic mice (CD45.1 or CD45.1.2) express a Vα2Vβ5 TCR heterodimer that recognizes a peptide derived from $OVA_{(257–264)}$ (OVAp) presented by $H\text{-}2K^b$.

To generate HP-memory populations, 10^6 $CD44^{low}$ OT-I cells (CD45.1) were sorted and adoptively transferred into B6 hosts rendered lymphopenic by sublethal irradiation (600 rads) 24 h prior. Cells were allowed to undergo homeostatic proliferation for at least 30 days before subsequent transfers. For generation of true-memory, 10^6 OT-I (CD45.1.2) cells were adoptively transferred into naive mice and infected with 5000 colony-forming units *Listeria monocytogenes* expressing OVA (Lm.OVA) i.v.; 30 days were allowed to pass before subsequent transfers. Before the second adoptive transfer into naive B6 mice, lymphocytes from spleen and lymph nodes were pooled and depleted of B and $CD4^+$ T cells using MACS. Cells (1×10^5–8×10^5) were transferred per mouse unless otherwise specified; similar results

were obtained for this range. Each of the different experimental groups received the same total number of OT-I T cells. Mice were rechallenged with 10^5 colony-forming units Lm.OVA, immunized with 100 μg OVAp/50 μg LPS, or left uninfected. Where indicated, lymphocytes from pooled spleen and lymph nodes were labeled with CFSE (10 μM final concentration; Molecular Probes) for 10 min at 37°C in PBS 0.1% BSA.

To inhibit CD62L-mediated entry into lymph nodes, 200 mg anti-CD62L (MEL-14) were administered i.p. ~4 h before adoptive transfer of memory cells. The next day, 200 mg Ab were administered i.p. ~4h before infection and thereafter each day. Rat IgG2a κ isotype or PBS was administered concurrently to control mice with similar results to untreated hosts. For cytokine complexes, IL-7 was precomplexed with an anti-IL-7 mAb (500-M07 PeproTech) and IL-15 was precomplexed with its soluble IL-15-receptor-α as previously described and administered i.p on days 3–7 of infection (11,12).

Lymphocytes were isolated from lung and liver, as previously described (13) with minor modifications. Mice were euthanized with CO_2 and perfused with PBS. Following collagenase digestion, cells were resuspended in Hanks' balanced salt solution, 5 mM EDTA, and 2% bovine growth serum, and layered on Ficoll-Paque Plus solution (Amersham Biosciences) and separated according to manufacturer's instructions. Intraepithelial lymphocytes were isolated as previously described (13) with a modified protocol. After incubation with 1 mM dithioerythritol, tissue was incubated at 37°C with Hanks' balanced salt solution and 1.3 mM EDTA for 30 min and layered over Ficoll.

Flow cytometry

Following secondary challenge, single cell suspensions were prepared from spleen and lymph node lysates. Fc receptors were first blocked with unconjugated mouse Ab to CD32/16 (2.4G2). The following Abs were used for phenotypic analysis: CD44 (IM7), CD62L (Mel-14), CD122 (TM-β1), CD127 (A7R34), LY6C (AL-2), CD43 (1B11), CXCR3 (R&D Systems cat. no. FAB1585P), CD27 (LG.759), CD49d (R1-2), KLRG1 (2F1), PD-1 (J43), CD132 (4G3), CD45.1 (A20), CD45.2 (104), and CD8α (53-6.7). All Abs are available commercially from eBioscience or BD Pharmingen unless otherwise noted. To detect apoptosis, allophycocyanin-conjugated annexin V/annexin buffer (Invitrogen) and 7-aminoactinomycin D (Invitrogen) were used. TUNEL staining was performed using the FragEL DNA fragmentation detection kit (Calbiochem) according to manufacturer's instructions. In short, cells were stained with surface Abs then fixed in PBS with 1% paraformaldehyde. Following a wash in PBS and 0.2% Tween 20, fluorescent TdT mix was added and incubated for 1.5 h. To measure in vivo proliferation, 1 mg BrdU (Sigma-Aldrich) was injected i.p into mice 15 h before sacrifice on indicated days. Splenocytes or lymph node cells were stained according to instructions from the BrdU flow kit (BD Biosciences). All samples were run on FACSCalibur or FACSAria (BD Biosciences). FlowJo software (TreeStar) was used for analysis.

mRNA array

SABioscience's quantitative PCR array (qPCR; cat. no. PAMM-022) was used to compare the relative levels of cDNA between HP- and true-memory OT-I cells 6 days after infection from sorted, pooled spleen cells. mRNA was extracted using TRIzol (Invitrogen) and cDNA was generated using the RT^2 first strand kit (SABioscience). Primers for mouse CXCR5 and CCR7 and the RT^2 SYBR Green/ROX PCR master mix were obtained from SABioscience. For each set of triplicates, the mean value of each gene was calculated using the $\Delta\Delta C_t$ method in comparison with the housekeeping gene.

Immunofluorescence

Freshly harvested tissues were soaked in 30% sucrose overnight and embedded in OCT. Six-micrometer-thick tissue sections were cut and fixed in acetone (–20°C). Sections were blocked in a solution of 10% BSA, 2.5% normal goat serum, 2.5% normal donkey serum, and fish scale gelatin. Tissue sections were then incubated with combinations of conjugated anti-mouse CD45.1, anti-rat Thy1.1/CD90 (OX-7), anti-mouse B220 (RA3-GB2), anti-mouse CD8a, anti-mouse CD4 (GK1.5) or anti-mouse CD11c (N418), followed by incubation with secondary mAb Alexa Fluor 546 streptavidin. Sections were mounted using Invitrogen ProLong Gold anti-fade reagent. Images were taken with an Olympus FV1000 confocal microscope with five laser lines at wavelengths of 405, 458, 488, 515, 543, and 647 nm, using 10× and 20× air objectives. Images were analyzed using ImageJ.

Results

True-memory cells out-compete HP-memory CD8$^+$ T cells during secondary infection

To compare HP- and true-memory T cell responses to Ag, we set up an adoptive transfer system where we could observe the response of both congenically marked populations with identical Ag specificity in the same host (Fig. 1*A*). HP-memory cells were generated by sorting CD44^{low}, naive OT-I TCR transgenic CD8$^+$ cells (CD45.1) and transferring them into sublethally irradiated B6 mice (CD45.2). Alternatively, true-memory cells were generated by transferring naive OT-I T cells (CD45.1.2) into B6 hosts followed by infection with recombinant Lm.OVA. Both populations ultimately possessed similar surface phenotypes for all markers tested with the exception of CD49d (supplemental Fig. S1).[4]

To study the behavior of the HP- and true-memory cells during infection, three experimental groups (a 1:1 mix of both populations, HP-memory alone, or true-memory alone) were transferred into new B6 hosts (Fig. 1*A*) and infected with Lm.OVA 1 day later. For all three groups, the total number of transferred OT-I T cells was equal; the single transfers received only HP- or true-memory cells and the mixed transfer received half the number of HP- and true-memory cells each for the same total number of cells. The co-transfer allowed us to observe how well the HP- and true-memory cells competed for resources and space during infection. The accumulation of each subset was monitored by FACS in the PBL and spleen. Both subsets responded to infection and underwent significant expansion (Fig. 1, *B–F*). However, in the case of the co-transfer, the true-memory cells displayed increased expansion and formed more secondary memory than the HP-memory cells (Fig. 1*B*), despite the earlier expansion of HP-memory cells. This early accumulation did not persist and the HP-memory cells ultimately generated fewer secondary memory cells. Comparing the number of cells recovered from spleen on day 5 of infection we found that 3.5×10^7 true-memory cells were recovered from the mixed transfers and 4.1×10^7 true-memory cells were recovered from the single transfers, indicating similar or greater expansion by the cells in mixed transfers (Fig. 1*F*). By day 11 of infection, similar numbers of effector/memory cells derived from true-memory donor cells were found in both transfer groups (~1×10^7 cells). In contrast, the HP-memory cells expanded less at day 5 when transferred with true-memory cells than in the single transfer group (2.2×10^7 cells for single transfer vs 0.9×10^7 for mixed transfer) and this was reflected in the number of effector/memory cells on day 11 (2.2×10^7 for single transfer and 0.2×10^7 for mixed transfer) (Fig. 1*F*). Thus, the expansion of true-memory cells was not altered significantly in the presence of HP-memory cells, but HP-memory cells ultimately showed diminished expansion in the presence of true-memory cells.

[4]The online version of this article contains supplemental material.

Similar results were observed during i.v. infection with vesicular stomatitis virus expressing OVA, an infection that is dependent on lymph nodes for priming, and when using P14 transgenic HP- and true-memory $CD8^+$ T cells responding to lymphocytic choriomeningitis virus administered i.p. (supplemental Fig. S2, *A* and *B*). Thus, the inability of HP-memory to compete with true-memory was not pathogen, route, or TCR specific. Of note, TRAIL-deficiency (6) did not rescue the ability of HP-memory cells to compete efficiently with true-memory T cells (supplemental Fig. S2*C*) and results were similar when congenic markers were flipped on the memory subsets (data not shown).

In the absence of a competing memory subset, the HP-memory response largely mirrored that of the true-memory cells, accumulating to similar levels and forming equivalent amounts of secondary memory in the PBL (Fig. 1, *C*, *E*, and *F*). There were minor differences in the contraction phase, where the HP-memory peaked earlier than the true-memory cells; however, they consistently formed robust secondary memory. The differences observed in the PBL between the single and competing memory cell transfers were reflected in the splenic analysis (Fig. 1, *D* and *E*).

These results raised the possibility that the HP-memory cells were not able to compete well with true-memory, despite their ability to expand, protect, and form secondary memory, when they act as the sole Ag-specific population. To assess the ability of the HP-memory to compete with other T cell subsets, we compared their ability to respond to infection with naive cells bearing the same TCR specificity after infection (Fig. 1, *G* and *H*). The HP-memory cells expanded first, and to a greater degree, and formed more secondary memory than naive T cells in both single and co-transfer experiments did (Fig. 1, *G* and *H*). Interestingly, the ability of HP-memory cells to outcompete naive T cells was not as robust as the true-memory subset, which formed a greater percentage of secondary memory when mixed with naive T cells (Fig. 1*I*). Thus, the HP-memory out-compete naive cells of the same specificity by providing more rapid expansion, greater secondary memory formation (Fig. 1), and enhanced protection (6).

We also analyzed whether the proliferation and death rate of the true-memory cells were affected by the presence of the HP-memory cells. Proliferation was monitored by BrdU incorporation on days 4–7 after infection. No significant difference was observed between the two memory subsets, but in both the spleen and lymph nodes, the true-memory cells consistently tended to incorporate more BrdU than their HP-memory counterparts (supplemental Fig. S3, *A* and *B*). Although moderate, this difference could translate into the significant decrease in accumulation seen in the PBL by HP-memory (Fig. 1*B*). The initial discrepancy would be magnified as effector cells proliferate quite extensively (four to six divisions per day) (14). Death of donor cells was measured by TUNEL and Annexin-V flow cytometry assays (supplemental Fig. S3, *C–F*) and no significant trends were observed.

Taken together, these data suggest that during infection, HP-memory cells are at a disadvantage when competing with their true-memory counterparts for shared resources, despite their ability to out-compete naive T cells. Thus, we find that although the HP-memory population is phenotypically and functionally similar to true-memory, it is not an exact substitute.

Localization of HP-memory vs true-memory $CD8^+$ T cells during infection

To distinguish whether the failure of the HP-memory cells to accumulate in spleen and blood during co-transfer was caused by altered localization rather than defective expansion, we examined multiple tissues for the presence of both subsets following co-transfer. Before infection, the HP- and true-memory cells had similar access to peripheral tissues displaying a 1:1 ratio in all tissues examined (Fig. 2*A*). This implies that initially, the HP-memory subset had equal access to Ag compared with the true memory cells. Interestingly, after infection we observed that the ratio of transferred cells favored the true-memory subset by 3–4-fold in all

tissues evaluated, with the exception of the lymph nodes (Fig. 2, *A* and *B*). Between days 4 and 5 of infection, it became evident that the true-memory possessed an advantage over the HP-memory subset, and this difference was sustained through day 30 of infection. In striking contrast to the other tissues, HP-memory cells were the predominant population in the lymph nodes early in the response and beyond into the memory phase (Fig. 2, *A* and *B*). The preference of HP-memory cells for homing to the lymph nodes correlated with their rapid up-regulation of CD62L, which facilitates lymph node entry (15). Before infection, the co-transferred HP- and true-memory subsets demonstrated equivalent trafficking (Fig. 2*A*) and possessed similar CD62L levels (supplemental Fig. S1). Initially after infection, both HP- and true-memory expressed low levels of CD62L (Fig. 2*C*). However, by day 6, more than 50% of the HP-memory cells were $CD62L^{high}$ compared with ~10% of the true-memory cells (Fig. 2*C*). Of note, both $CD62L^{high}$ and $CD62L^{low}$ true-memory populations can out-compete HP-memory cells with similar efficiency, suggesting that competitive fitness is not dependent on functional differences between central and effector memory subsets (data not shown). Additionally, on day 6 of infection, the surface phenotype of the effector cells generated from HP-memory cells showed a moderate increase in CD127 and CD27 and a decrease in KLRG1 expression compared with effectors derived from true-memory cells (supplemental Fig. S4).

To determine whether the increased numbers of HP-memory cells in the lymph nodes offset a loss in spleen and peripheral tissues, we compared donor cell recovery after co-transfer and infection. By day 7 of infection, more than 2-fold more true-memory than HP-memory cells accumulated in spleen and all recoverable lymph nodes (Fig. 2*D*), suggesting that the loss of HP-memory in the spleen and tissues represented diminished accumulation and formation of secondary memory rather than lymph node relocation. Furthermore, we treated mice with anti-CD62L to block lymphocyte trafficking to lymph nodes during infection. Overall, $CD8^+$ T cell numbers decreased for both memory subsets in the lymph nodes (Fig. 2*E*, *left*), indicating effective Ab blocking, but this did not restore HP-memory cell numbers to the levels of true-memory cells present in the spleen (Fig. 2*E*, *right*). Although CD62L expression may have played a role in the alternative localization pattern of the HP-memory cells to the lymph nodes, it did not explain the systemic failure of HP-memory cells to accumulate in all of the other tissues.

HP-memory cells display a distinct localization pattern in the spleen after infection

We next examined HP- and true-memory $CD8^+$ T cell localization within the spleen during infection. Early on (day 2), HP- and true-memory cells localized to the periarteriolar lymph sheath (PALS) indicated by colocalization with $CD4^+$ T cells (Fig. 3, *A*–*C*). $CD11c^+$ cells were found in the PALS, but also accumulated peripherally to the marginal zone (MZ) in the red pulp (RP). We did not observe any noticeable differences in localization by the HP- and true-memory cells between days 1–2 of infection (Figs. 3 and S5). This indicated that the HP-memory cells were initially located appropriately for Ag recognition, consistent with Fig. 1*A*, where no defect in expansion was observed during the first 4 days of infection.

However, it was evident by day 5 of infection that the true-memory cells had localized to the MZ/RP with the $CD11c^+$ cells (Fig. 3*D*). In contrast, the HP-memory cells remained largely in the PALS. This striking difference between HP- and true-memory cell localization within the spleen was accentuated as the infection progressed (Figs. 4 and S5). By day 5 of infection, the true-memory cells were already largely absent from the PALS and accumulated in the RP/MZ along the edge of the B cell follicle (Fig. 4*A*). In contrast, the HP-memory cells were still abundant in the PALS and were also scattered throughout the RP and even the B cell zone. HP-memory cells were rarely found in clusters of more than two or three cells and only a portion colocalized with the true-memory cells along the B cell follicle edge (Fig. 4). At 10

days after infection, significant numbers of HP-memory cells remained in the PALS whereas true-memory cells were observed mainly in the RP/MZ regions (Figs. 4*A* and S5).

Under conditions of competition, the HP-memory cells still localized appropriately to the PALS at the beginning of the response. However, trafficking and localization of the HP-memory cells differed dramatically from true-memory cells later in the infection, indicating that HP- and true-memory cells received distinct signals at some point in the response. Single transfer of HP-memory cells not competing with true-memory cells demonstrated an intermediate phenotype, with increased numbers of cells in the RP along the B cell follicle edge during the peak of the response but not to the extent exhibited by the true-memory cells (supplemental Fig. S6).

Differential mRNA expression for chemokine receptors by HP-memory cells

The differential trafficking by the HP-memory cells (Fig. 4) led us to investigate chemokine receptor expression by the two memory subsets using a chemokine/chemokine receptor qPCR array. On day 6 of infection, when there were clearly significant differences between the localization of the subsets, HP- and true-memory cells were sorted from pooled spleens of co-transfer recipients. Relative mRNA levels for 84 genes, comprised primarily of chemokines and chemokine receptors, were evaluated by qPCR. Fig. 5 summarizes the target genes that have 2-fold or greater difference in expression between HP- and true-memory cells. Of particular interest were the chemokine receptors CXCR4, CXCR5, CXCR7, and CCR7, which have roles in lymphocyte homing in secondary lymphoid organs (Fig. 5). The HP-memory cells expressed ~10-fold more CXCR5 mRNA than the true-memory controls (Fig. 5, *A* and *B*, *left*). Although the function of CXCR5 on $CD8^+$ T cells is not well characterized, CXCR5 expression on $CD4^+$ Th cells mediates their localization to the B cell follicle (16). CXCR4 and CXCR7 both bind to CXCL12, a chemokine found in the B cell zone, but are not characteristically expressed by $CD8^+$ T cells (17,18). CCR7 was also up-regulated on HP-memory cells (Fig. 5, *A* and *B*, *right*) and mediates T cell and dendritic cell (DC) homing and positioning in the T cell zone. CCR7 ligands are known to be secreted by DC, macrophages, and stromal cells in the T cell zone (16). Increased expression of CCR7 and chemokine receptors that mediate homing to the B cell follicle may explain why a significant portion of the HP-memory cells were retained in the PALS and B cell zone and why they displayed disorganized localization compared with the true-memory cells. Interestingly, the HP-memory cells also showed increased chemotaxis to CCR7 ligands compared with true-memory cells (supplemental Fig. S7), suggesting greater expression of a functional receptor.

Competition between HP- and true-memory cells cannot be fully rescued by provision of excess Ag or survival cytokines

Although many signals are necessary to support the expansion of T cells during infection, Ag and cytokines were obvious candidates for the basis of competition between the HP- and true-memory subsets, particularly considering the differential localization of the two cell types. To provide Ag in excess and without bias of professional APCs, we compared the expansion of HP- and true-memory cells in response to OVAp and LPS administered i.v. (Fig. 6*A*). Here, we found that the HP-memory cells were still at a disadvantage compared with true-memory cells, indicating that the defect was not the result of a failure to compete for Ag in the early phase of the immune response.

The common γ-chain cytokines IL-7 and IL-15 both support accumulation of $CD8^+$ T cells during contraction of the immune response (1,12). Although HP- and true-memory cells displayed similar expression of these cytokine receptors (Fig. S1), it was possible that HP-memory cells did not compete well for limiting amounts of cytokines or gain access to the cytokine signals in light of their altered localization. We tested whether increasing the amount

of cytokine available by administering IL-7 or IL-15 complexes (12) could rescue the HP-memory cells. Addition of exogenous IL-7 and IL-15 complexes led to an increase in numbers of both memory subsets compared with PBS-treated controls (Fig. 6), and did not alter the kinetics of HP-memory expansion or secondary memory formation (Fig. 6). However, the differences in the ratio, percentage, and number of true- vs HP-memory cells revealed a partial rescue in the accumulation of the HP-memory cells following treatment with IL-7 complexes (Fig. 6). The addition of the IL-15/IL-15Rα complexes (Fig. 6) boosted cell numbers of both memory subsets, but the HP-memory subset still expanded less than the true-memory.

HP-memory cells undergo diminished basal homeostatic proliferation

As memory T cells survive for extended periods of time while undergoing a slow turnover in the absence of Ag, we were also interested in whether HP-memory cells competed efficiently with true-memory cells during this process of basal homeostatic proliferation. In a lymphoreplete environment without Ag, basal levels of IL-7 and IL-15 promote survival and homeostatic turnover (1). We transferred HP- and true-memory at a ratio of 1:1 or alone into naive, congenically distinct hosts, and the percentage of donor cells among the PBL was monitored for >100 days (Fig. 7). In mixed transfers, the true-memory subset slowly accumulated and accounted for the majority of the donor cells (Fig. 7*A*). The two subsets started off at an ~1:1 ratio, but by days 40–60 after transfer, the true-memory cells began to show an advantage over the HP-memory cells. By 120 days post transfer, CFSE dilution by transferred memory cells in the spleen showed that both populations underwent multiple rounds of division, but the true-memory underwent two to three more divisions than the HP-memory cells over the course of the experiment (Fig. 7*B*). This difference in basal homeostatic proliferation was reflected by the increased proportion of true-memory in the donor population (Fig. 7*D*), while the HP-memory subset remained relatively stable (Fig. 7*C*). Interestingly, a similar accumulation by the HP-memory was observed when the subsets were transferred separately (Fig. 7, *E* and *F*).

Thus, in the absence of infection, the HP-memory cells possessed the ability to survive and compete for resources when in competition with true-memory cells, but they did not divide and accumulate to the levels observed by the Ag-experienced memory T cells. The ability of HP-memory cells to survive in the absence of infection is not affected by the presence of co-transferred true-memory cells (Fig. 7, *C* and *E*), perhaps because they were required to compete with host cells within the memory compartment for cytokines or niches irrespective of whether OT-I true-memory cells were present.

Discussion

The memory T cell compartment is composed of heterogeneous phenotypic and functional subsets, including cells that acquired these properties not only by Ag exposure but also as a result of HP. Lymphopenia-induced HP occurs early in neonatal life, following some acute and chronic infections, and can be the result of lymphotoxic therapies. These memory-cell doppelgangers provide improved protection over the naive response (6), but their integration into the memory T cell compartment and possible interference with the immune response of true-memory cells has not been investigated. Acting as the sole Ag-specific population, the HP-memory cells respond to infection and form a secondary memory population much like true-memory cells (Fig. 1, *C* and *E*). However, in the presence of Ag-experienced cells of the same specificity, the HP-memory cells were outcompeted in both basal conditions and secondary infection (Figs. 1, *B* and *D*, and 7).

Early on, the HP-memory cells colocalized with and expanded similarly to their true-memory counterparts, but contracted earlier and to a greater extent (Figs. 1, 3, and 4). Coinciding with this contraction, the HP-memory cells displayed altered localization compared with true-

memory cells–remaining in the PALS, infiltrating the B cell follicle, and exhibiting a diffuse pattern (Fig. 4). Thus, the HP-memory subset contributed less to the secondary memory population than the true-memory subset, revealing a competitive hierarchy whereby true-memory cells respond more efficiently than HP-memory cells and both memory subsets out-compete naive T cells of the same specificity during infection.

Signals promoting HP- and true-memory cell differentiation are quite distinct. The initial naive $CD8^+$ T cell response to infection and subsequent formation of a memory population requires TCR-mediated recognition of pathogen-derived peptide/MHC class I complexes on professional APCs, costimulatory signals, and inflammatory cytokines (1). In contrast, acquisition of a memory phenotype by naive cells during lymphopenia-induced proliferation is triggered by low-affinity interactions with self-peptide/MHC complexes and IL-7 (2) and is costimulation independent (3,19). Previous experiments found that HP-memory cells shared a similar gene-expression profile with true-memory cells (7) and displayed true-memory phenotypic and functional characteristics (2,3,6). Thus, it was surprising that HP-memory cells deferred to the true-memory cells during infection.

What is the basis for competition between HP- and true-memory cells during infection? Access to APCs, which influence the level or duration of Ag exposure (20) as well as costimulation or cytokine availability, contributes to the degree of stimulation and subsequent formation of secondary memory cells (21). Both IL-7 and IL-15 mediate memory cell survival during contraction and were thus candidates for moderating the advantage observed by true-memory cells (1,12). Provision of either cytokine during infection was unable to fully rescue HP-memory accumulation; however, IL-7 complexes did improve the accumulation of HP-memory cells (Fig. 6). Thus, the paucity of IL-7 or IL-15 is not the sole basis for competition, and the signals they mediate fail to completely overcome the HP-memory defect.

Early after infection, HP- and true-memory cells localized in the PALS, along with the DC (Fig. 3*A*). This was an opportunity for HP-memory cell Ag exposure as $CD11c^+$ cells mediate Lm.OVA transit into the PALS and $CD8^+$ T cell presentation (22). Indeed, the HP-memory cells adopted phenotypic changes typical of Ag exposure (supplemental Fig. S4) and initial expansion rivaled that of the true-memory cells (Fig. 1*B*). Furthermore, providing abundant Ag by i.v. OVAp/LPS immunization or OVA-expressing LPS B cell blasts did not rescue the HP-memory cells (Fig. 6*A* and data not shown). Thus, we find no evidence that Ag is the limiting factor favoring the true-memory cells. However, we do see that HP-memory cells up-regulate CD62L expression rapidly and have lower levels of KLRG1 after infection (Figs. 2*C* and S4), evidence that they may receive an attenuated antigenic signal (23,24).

Localization of the HP-memory within the spleen was dramatically altered by day 4 of infection (Figs. 3*B* and 4). The true-memory cells were located primarily in the RP, where significant CD11c staining was also observed (Fig. 3*D*). In contrast, the HP-memory cells were scattered throughout the PALS, B cell zone, and RP (Figs. 3 and 4), likely due to aberrant expression of chemokine receptors that direct cells to the B cell zone (CXCR4, CXCR5, CXCR7) or retain cells in the T cell zone (CCR7) (Fig. 5). Thus, it is conceivable that the HP-memory cells failed to receive signals that alter chemokine receptor expression early in the response, directly resulting in poor memory formation or a failure to receive additional signals later in the response due to their inappropriate localization. Alternatively, the failure to compete efficiently with true-memory cells may be unrelated to the differential localization. It has been shown that $CD8^+$ memory formation, but not expansion, is dependent on ICAM-1 expression by DC, suggesting sustained contacts between the T cell and APCs influence how efficiently memory formation occurs (25). HP-memory cells expressed normal levels of LFA-1, the ligand for ICAM-1 (data not shown), but did have lower levels of CD49d, an integrin expressed by activated T cells, which mediates cell adhesion and trafficking. However, blocking CD49d

(26) did not eliminate the true-memory advantage or significantly alter localization (data not shown).

Many aspects of the $CD8^+$ T cell response are determined or programmed early after antigenic stimulation, including degree of proliferation, timing of contraction, and ability to respond in a secondary infection (21). We observed that the HP-memory response was similar to the true-memory cells when they were not in direct competition (Fig. 1, *C* and *E*). However, several lines of evidence suggested that, in addition to their inability to compete and express chemokine receptors correctly during infection, HP-memory cells do not undergo the full memory program during lymphopenia-induced proliferation. HP-memory cells underwent slower turnover than true-memory cells, comprising less of the memory compartment over time (Fig. 7). Further, even when responding without competition, the HP-memory cells still showed some signs of chaotic localization (Fig. S6) but received adequate signals for secondary memory formation (Fig. 1, *C* and *D*). The intermediate localization pattern by HP-memory cells in the transfer lacking competition agreed with the findings that chemokine receptor mRNA expression was not fully rescued and chemotaxis to CCR7 ligands was retained in the single transfer (Fig. S7). Together, these data indicate the presence of true-memory cells exacerbates a defect in the ability of HP-memory cells to directly access signals that regulate chemokine receptor expression and/or secondary memory formation.

Taken together, our results show that HP-memory T cells provide improved protection over naive T cell responses in the absence of competition, but importantly do not compromise responses of the tried-and-true Ag-experienced memory population. Thus, homeostatic mechanisms ensure that those memory-like cells arising during lymphopenia are not retained at the expense of pathogen- or vaccine-induced memory cells, suggesting that generation of these cells following lymphotoxic therapies will not erode recall responses.

Supplementary Material

Refer to Web version on PubMed Central for supplementary material.

Acknowledgments

We thank Dr. Warren D'Souza for helpful discussions and Pedro Lee for advice regarding histology. Additionally, we acknowledge Drs. Schoenberger, Koehn, Hedrick, and Surh for sharing mice, reagents, and advice. Finally, our appreciation to Drs. Rubinstein, D'Cruz, and Werneck for critical review of this manuscript.

References

1. Marsden VS, Kappler JW, Marrack PC. Homeostasis of the memory T cell pool. Int. Arch. Allergy Immunol 2006;139:63–74. [PubMed: 16319493]
2. Goldrath AW. Maintaining the status quo: T-cell homeostasis. Microbes Infect 2002;4:539–545. [PubMed: 11959509]
3. Cho BK, Rao VP, Ge Q, Eisen HN, Chen J. Homeostasis-stimulated proliferation drives naive T cells to differentiate directly into memory T cells. J. Exp. Med 2000;192:549–556. [PubMed: 10952724]
4. Tan JT, Dudl E, LeRoy E, Murray R, Sprent J, Weinberg KI, Surh CD. IL-7 is critical for homeostatic proliferation and survival of naive T cells. Proc. Natl. Acad. Sci. USA 2001;98:8732–8737. [PubMed: 11447288]
5. Khoruts A, Fraser JM. A causal link between lymphopenia and autoimmunity. Immunol. Lett 2005;98:23–31. [PubMed: 15790505]
6. Hamilton SE, Wolkers MC, Schoenberger SP, Jameson SC. The generation of protective memory-like $CD8^+$ T cells during homeostatic proliferation requires $CD4^+$ T cells. Nat. Immunol 2006;7:475–481. [PubMed: 16604076]

7. Goldrath AW, Luckey CJ, Park R, Benoist C, Mathis D. The molecular program induced in T cells undergoing homeostatic proliferation. Proc. Natl. Acad. Sci. USA 2004;101:16885–16890. [PubMed: 15548615]
8. Dummer W, Niethammer AG, Baccala R, Lawson BR, Wagner N, Reisfeld RA, Theofilopoulos AN. T cell homeostatic proliferation elicits effective antitumor autoimmunity. J. Clin. Invest 2002;110:185–192. [PubMed: 12122110]
9. Wu Z, Bensinger SJ, Zhang J, Chen C, Yuan X, Huang X, Markmann JF, Kassaee A, Rosengard BR, Hancock WW, Sayegh MH, Turka LA. Homeostatic proliferation is a barrier to transplantation tolerance. Nat. Med 2004;10:87–92. [PubMed: 14647496]
10. Selin LK, Brehm MA, Naumov YN, Cornberg M, Kim SK, Clute SC, Welsh RM. Memory of mice and men: $CD8^+$ T-cell cross-reactivity and heterologous immunity. Immunol. Rev 2006;211:164–181. [PubMed: 16824126]
11. Rubinstein MP, Kovar M, Purton JF, Cho JH, Boyman O, Surh CD, Sprent J. Converting IL-15 to a superagonist by binding to soluble IL-15Rα. Proc. Natl. Acad. Sci. USA 2006;103:9166–9171. [PubMed: 16757567]
12. Rubinstein MP, Lind NA, Purton JF, Filippou P, Best JA, McGhee PA, Surh CD, Goldrath AW. IL-7 and IL-15 differentially regulate $CD8^+$ T-cell subsets during contraction of the immune response. Blood 2008;112:3704–3712. [PubMed: 18689546]
13. Masopust D, Vezys V, Marzo AL, Lefrancois L. Preferential localization of effector memory cells in nonlymphoid tissue. Science 2001;291:2413–2417. [PubMed: 11264538]
14. Mempel TR, Henrickson SE, Von Andrian UH. T-cell priming by dendritic cells in lymph nodes occurs in three distinct phases. Nature 2004;427:154–159. [PubMed: 14712275]
15. Arbones ML, Ord DC, Ley K, Ratech H, Maynard-Curry C, Otten G, Capon DJ, Tedder TF. Lymphocyte homing and leukocyte rolling and migration are impaired in L-selectin-deficient mice. Immunity 1994;1:247–260. [PubMed: 7534203]
16. Muller G, Hopken UE, Lipp M. The impact of CCR7 and CXCR5 on lymphoid organ development and systemic immunity. Immunol. Rev 2003;195:117–135. [PubMed: 12969315]
17. Balabanian K, Lagane B, Infantino S, Chow KY, Harriague J, Moepps B, Arenzana-Seisdedos F, Thelen M, Bachelerie F. The chemokine SDF-1/CXCL12 binds to and signals through the orphan receptor RDC1 in T lymphocytes. J. Biol. Chem 2005;280:35760–35766. [PubMed: 16107333]
18. Allen CD, Ansel KM, Low C, Lesley R, Tamamura H, Fujii N, Cyster JG. Germinal center dark and light zone organization is mediated by CXCR4 and CXCR5. Nat. Immunol 2004;5:943–952. [PubMed: 15300245]
19. Prlic M, Blazar BR, Khoruts A, Zell T, Jameson SC. Homeo-static expansion occurs independently of costimulatory signals. J. Immunol 2001;167:5664–5668. [PubMed: 11698438]
20. Kedl RM, Kappler JW, Marrack P. Epitope dominance, competition and T cell affinity maturation. Curr. Opin. Immunol 2003;15:120–127. [PubMed: 12495743]
21. Prlic M, Williams MA, Bevan MJ. Requirements for CD8 T-cell priming, memory generation and maintenance. Curr. Opin. Immunol 2007;19:315–319. [PubMed: 17433873]
22. Aoshi T, Zinselmeyer BH, Konjufca V, Lynch JN, Zhang X, Koide Y, Miller MJ. Bacterial entry to the splenic white pulp initiates antigen presentation to $CD8^+$ T cells. Immunity 2008;29:476–486. [PubMed: 18760639]
23. Kaech SM, Wherry EJ. Heterogeneity and cell-fate decisions in effector and memory $CD8^+$ T cell differentiation during viral infection. Immunity 2007;27:393–405. [PubMed: 17892848]
24. Sarkar S, Kalia V, Haining WN, Konieczny BT, Subramaniam S, Ahmed R. Functional and genomic profiling of effector CD8 T cell subsets with distinct memory fates. J. Exp. Med 2008;205:625–640. [PubMed: 18316415]
25. Scholer A, Hugues S, Boissonnas A, Fetler L, Amigorena S. Intercellular adhesion molecule-1-dependent stable interactions between T cells and dendritic cells determine $CD8^+$ T cell memory. Immunity 2008;28:258–270. [PubMed: 18275834]
26. Craddock CF, Nakamoto B, Andrews RG, Priestley GV, Papayannopoulou T. Antibodies to VLA4 integrin mobilize long-term re-populating cells and augment cytokine-induced mobilization in primates and mice. Blood 1997;90:4779–4788. [PubMed: 9389694]

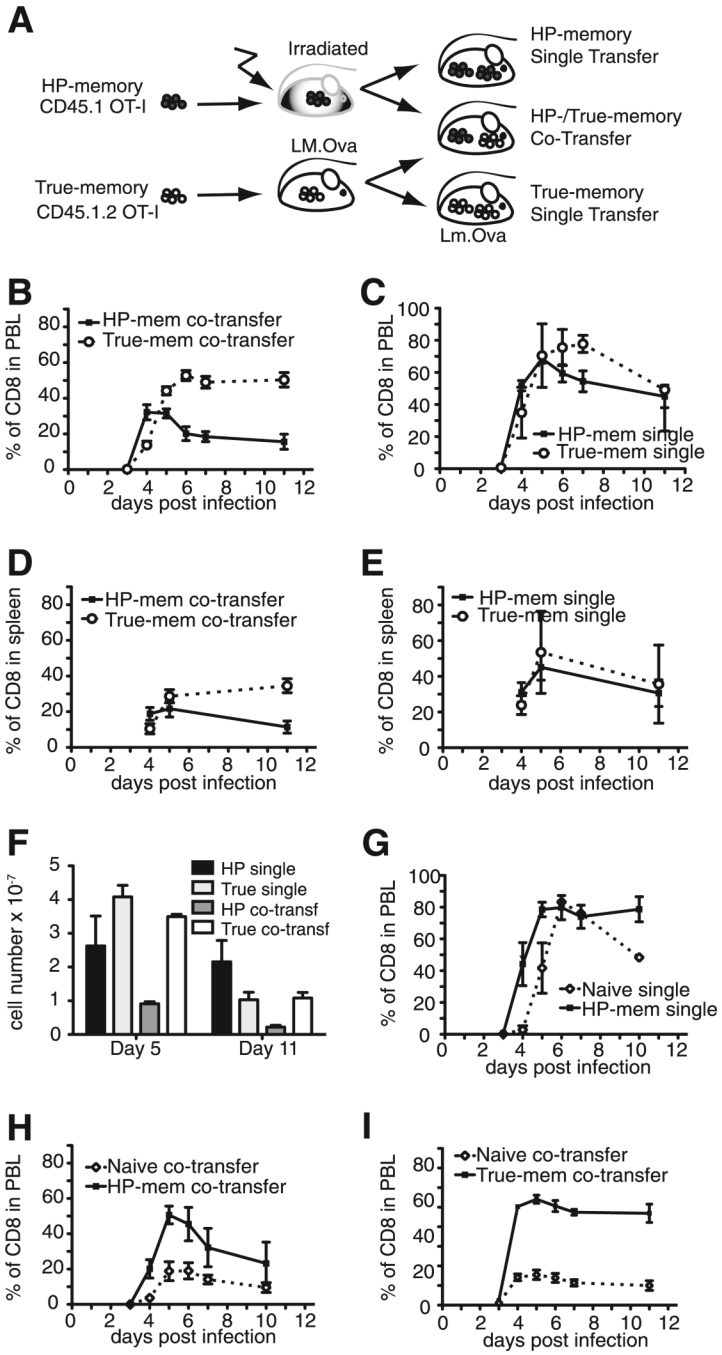

FIGURE 1.

True-memory $CD8^+$ T cells outcompete HP-memory cells during secondary infection. *A*, Generation of memory T cell subsets and experimental design. Immune response of the donor memory subsets was measured as a percentage of the total $CD8^+$ cells in the indicated tissue. *B*, Co-transfer: HP- and true-memory, PBL. *C*, Single transfer: HP- and true-memory, PBL. *D*, Co-transfer: HP- and true-memory, spleen. *E*, Single transfer: HP- and true-memory, spleen. *F*, Total cell numbers recovered from spleen for indicated transfer conditions. Co-transfer: naive OT-I and HP-memory, PBL. *G*, Single transfer: naive OT-I and HP-memory, PBL. *H*, Co-transfer: naive and HP-memory. Representative of >3 experiments ($n = 3$). Error bars indicate SD. *I*, Co-transfer: naive and true-memory. Mem, memory; transf, transfer.

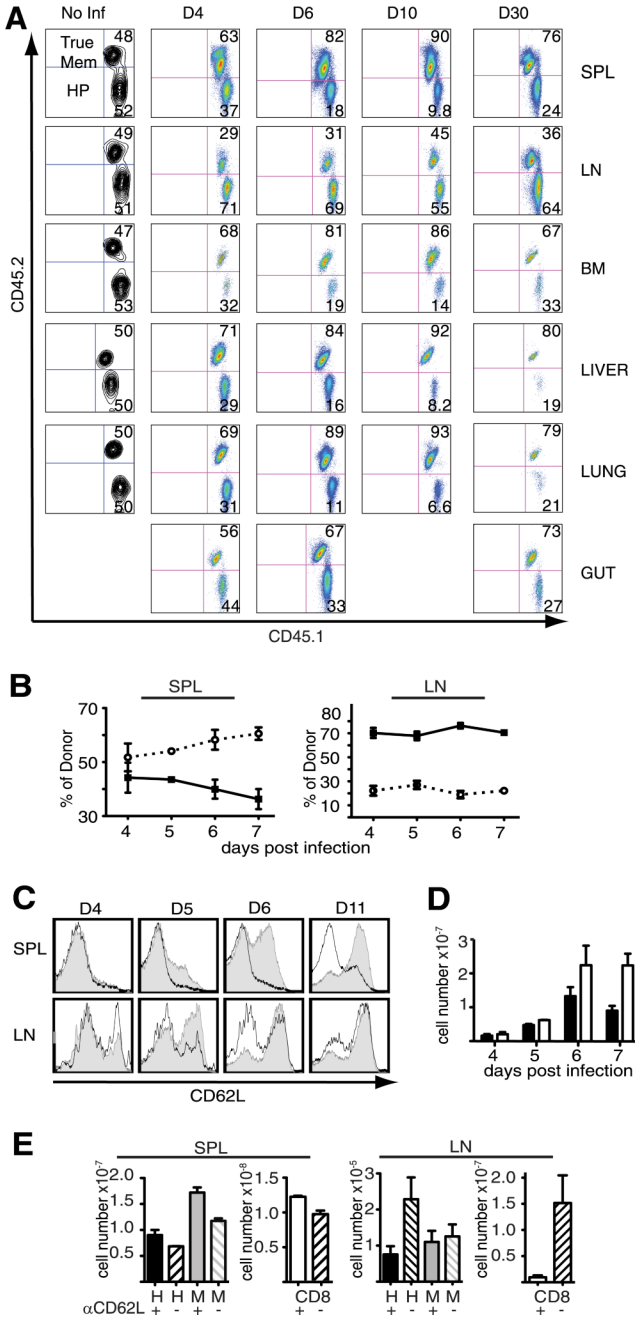

FIGURE 2.

Defect in HP-memory cell accumulation is not due to peripheral localization. The ratios of co-transferred memory subsets were monitored in the indicated tissues after Lm.OVA infection. *A*, Relative accumulation of the donor (CD45.1$^+$ CD8$^+$) subsets in the spleen (SPL), lymph nodes (LN), bone marrow (BM), liver, lung, and gut following infection. Memory subsets in the spleen and lymph nodes after infection: (*B*) percent of each donor memory subset (HP, solid line; true-memory, dotted line), (*C*) CD62L expression on co-transferred memory subsets (HP, gray; true-memory, white). *D*, Average total cell numbers from pooled spleen and all lymph nodes (HP, black; true-memory, white). *E*, Total cell numbers for donor HP- or true-memory cells from the spleen (*left*) and all recovered lymph nodes (*right*) following treatment with anti-CD62L or PBS (similar results obtained with isotype control). Host naive CD8$^+$ cell

numbers indicated in separate graphs (*right*). Representative of >3 experiments ($n = 3$). Error bars indicate SD. Mem, memory; Inf, infection; d, day; H, HP; M, true-memory.

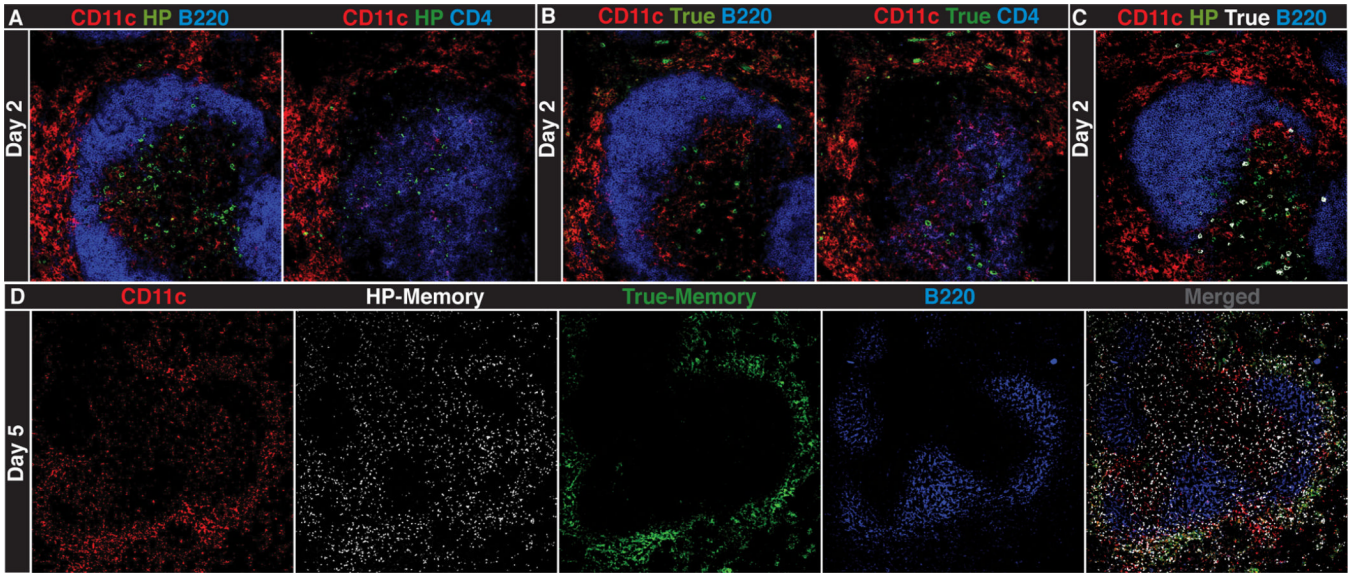

FIGURE 3.

Localization of HP- and true-memory cells relative to $CD11c^+$ cells. Confocal images of serial spleen sections from co-transfer recipients (day 2 of infection). Sections were stained for CD11c, B220, or CD4, and congenic markers for HP-memory (*A*), true-memory (*B*), and HP- and true-memory (*C*). *D*, Spleen (day 5) was stained for CD11c, both memory subsets, and B220 (10× magnification). Images are taken at 20× magnification unless noted. Representative of three experiments (n = 2–3) per time point.

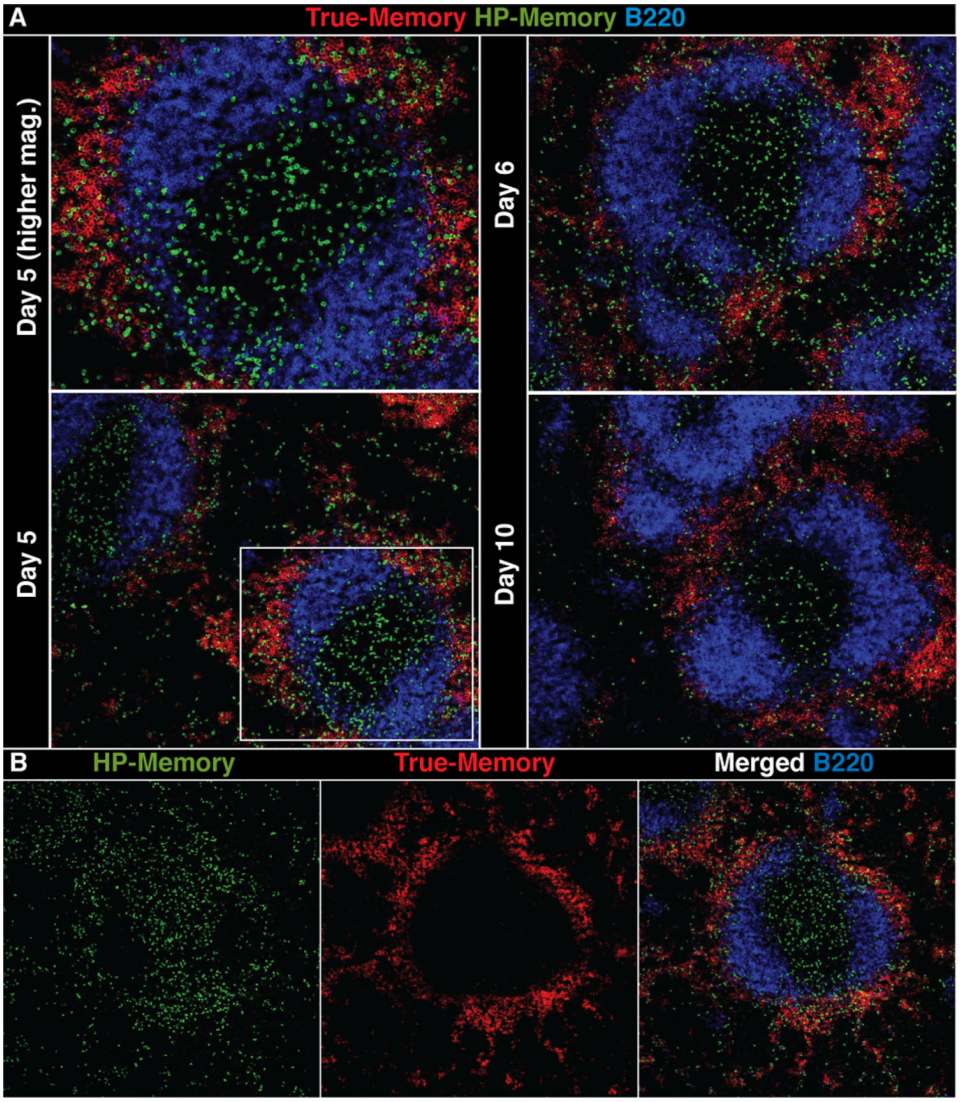

FIGURE 4.

HP- and true-memory cells display distinct localization and clustering in the spleen. *A*, Spleen sections of co-transfer recipients on days 5, 6, and 10. Stained for both memory subsets and B220. *B*, Panels with the indicated stains and merged image of spleen (day 5). Images are taken at 10× magnification. Representative of three experiments ($n = 3$) per time point.

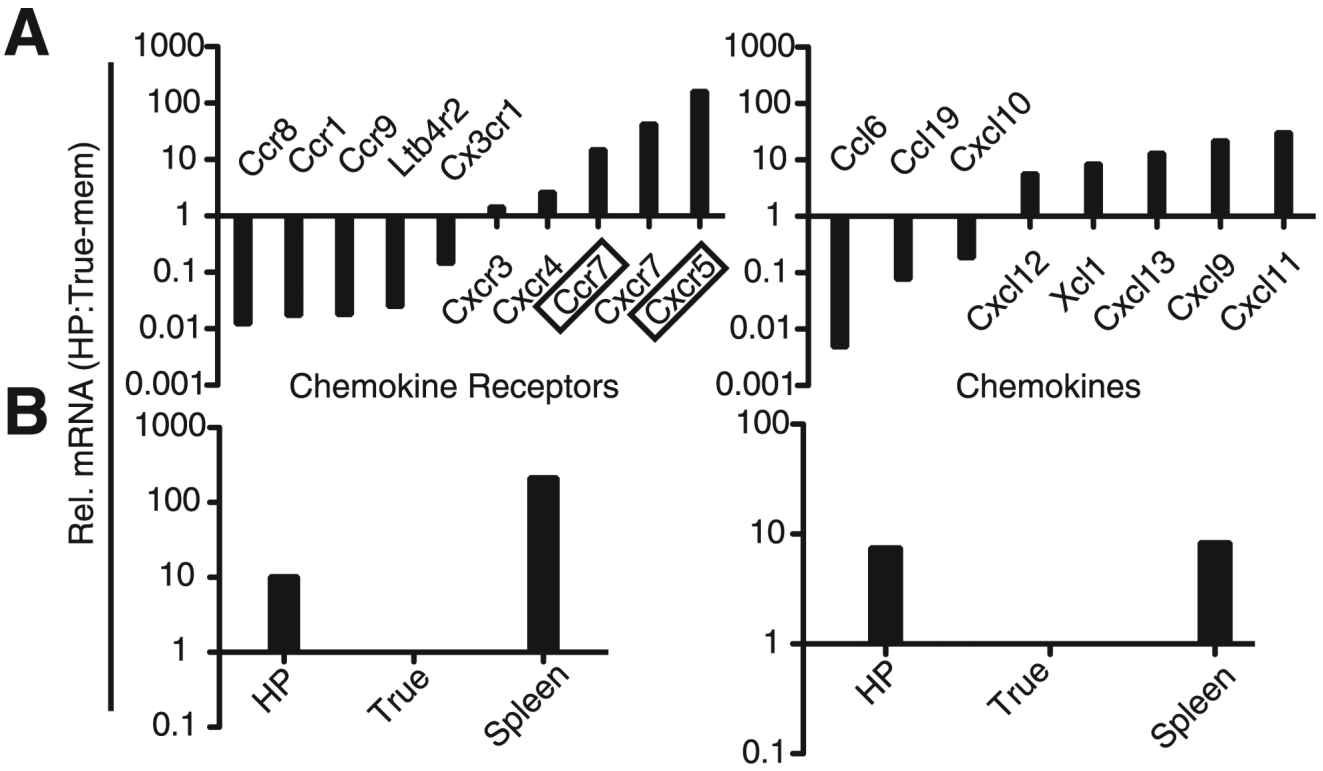

FIGURE 5.

mRNA levels of chemokines and chemokine receptors by HP- and true-memory cells. cDNA was generated from co-transferred HP- and true-memory cells sorted from pooled spleen (day 6). Relative (Rel.) mRNA levels for indicated genes were determined with a qPCR array and normalized to GAPDH. *A*, The transcripts displaying a 2-fold or greater difference in expression were listed and further divided into receptors (*left*) and chemokines (*right*). *B*, qPCR verification of CXCR5 (*left*) and CCR7 (*right*) mRNA levels. mRNA from total spleen used as a reference. Representative of two co-transfers tested >3 independent times.

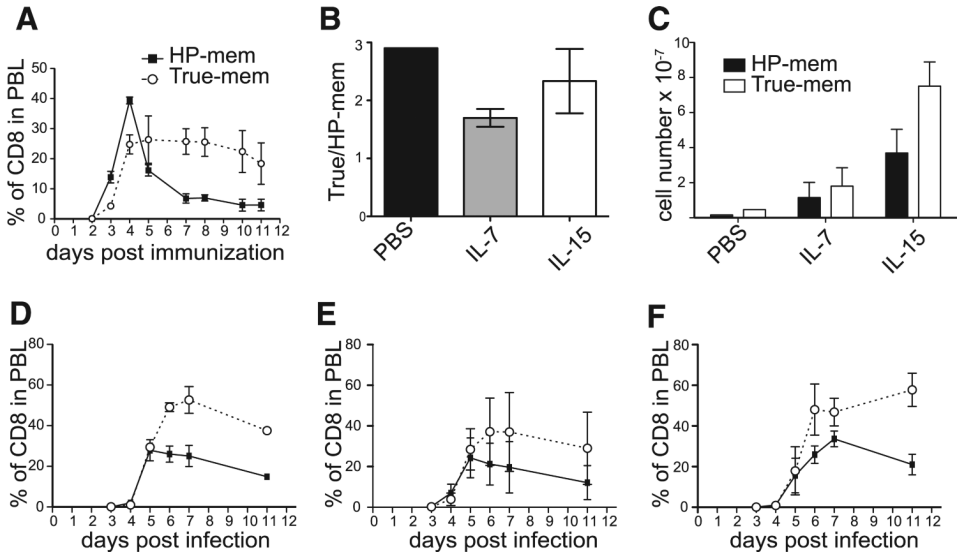

FIGURE 6.

The role of Ag and cytokines in the defective competition by HP-memory cells. *A*, Percentage of donor cells among total $CD8^+$ cells, PBL: OVAp, and LPS treated. *B*, Ratio of the percent of true-memory to HP-memory cells in spleen on day 10 of infection, recipients treated with PBS, IL-7/anti-IL-7 mAb, or IL-15/IL-15Rα complexes. *C*, Total cell number of each memory subset (day 10 Lm.OVA) treated with PBS (*D*), IL-7/anti-IL-7 mAb (*E*), and IL-15/IL-15Rα complexes (*F*). Representative of at least three experiments ($n = 3$). Error bars represent SD.

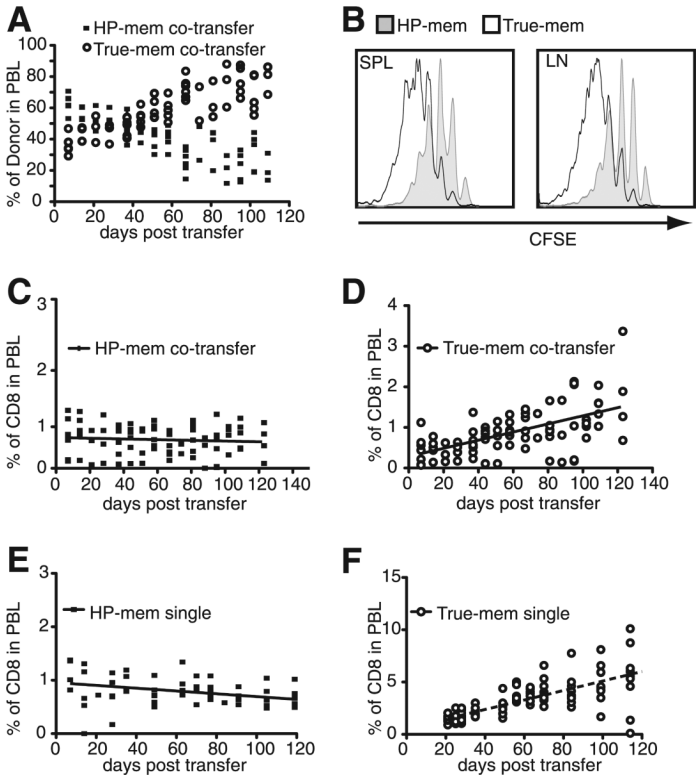

FIGURE 7.

True-memory cells accumulate and show increased basal homeostatic proliferation compared with HP-memory cells in the absence of infection. HP and true-memory subsets were monitored after transfer into naive B6 hosts without infection. *A*, Percentage of donor cells in PBL after co-transfer. *B*, CFSE detection of the co-transferred memory cells in the spleen and lymph nodes at 120 days post transfer. Percentage of the indicated subset among total $CD8^+$ T cells: (*C*) co-transfer, HP-memory; (*D*) co-transfer, true-memory; (*E*) single transfer, HP-memory; and (*F*) Single transfer, true-memory. Representative of two experiments ($n = 5$). Error bars indicate SD.